

Spectroscopy of bound excitons in cubic ZnS at moderate to high excitation densities

J. Gutowski, I. Broser, and G. Kudlek

Institut für Festkörperphysik der Technischen Universität Berlin, Hardenbergstrasse 36, D-1000 Berlin 12, Germany

(Received 17 June 1988)

We report on luminescence and excitation spectroscopy of bound excitons in cubic ZnS for moderate to high incident-light intensities. For the first time, the electronic fine structure of the ground state of the acceptor-exciton complex could be analyzed for two different acceptor centers, one of them being due to an iodine-related impurity. The electronic states of the complexes give rise not only to pronounced excitation resonances but also to intense resonant Raman scattering. For increasing excitation densities, the bound excitons are shown to remain the dominant excitonic feature in cubic ZnS until, for more than 100 kW/cm², a broadband emission begins to cover the whole investigated range; this emission is most probably due to electron-hole-drop creation.

I. INTRODUCTION

In recent times, the importance of bound-exciton transitions for the optical properties of II-VI compound semiconductors at high excitation densities became evident. Detailed investigations at Cd,¹⁻³ CdSe,² ZnTe,⁴ and ZnO (Ref. 5) demonstrated the complicated and highly efficient influence of these transitions on the typical high-density luminescence and absorption features of these compounds.

In contrast to that, rather little is known about bound excitons in ZnS, in particular for higher excitation densities. After bound excitons first had been proven to exist in hexagonal ZnS,⁶ they were also observed in cubic ZnS (Ref. 7) under electron-beam excitation (3 kW/cm² maximum). A broad and structured emission feature between 3.76 and 3.80 eV (the latter is the free *A*-exciton energy) was interpreted as being composed of seven bound-exciton transitions. They were attributed to bound-exciton complexes without further hints for a particular identification. Some additional bound-exciton lines were reported in Ref. 8, obtained for 20-keV electron-beam excitation. The only pulse laser measurements⁹ known to us showed few specific bound-exciton lines and edge-luminescence series which were attributed to a particular shallow-donor dopant. However, the excitation density was restricted to 0.8 kW/cm². The excitonic behavior for further increasing light densities has hardly been known up to now. Only Baltrameyunas and Kuokshtis¹⁰ observed one broad band emerging from a single bound-exciton line for growing excitation intensities of light from the fourth harmonic of a neodymium-doped yttrium aluminum garnet (Nd:YAG) laser. They interpreted this band as being due to electron-hole-drop (EHD) formation at 4.2 K, analogous to similar bands in ZnSe and ZnTe.¹¹

It is the purpose of this paper to contribute to the knowledge of the role of bound excitons in cubic ZnS at increased excitation densities. We performed luminescence and, for the first time, excitation spectroscopy of bound-exciton transitions for moderate to high excitation densities in the bound-exciton energy regime. It is shown

that a manifold of sharp emission lines occurs which can be assigned to neutral-acceptor-exciton complexes. Excitation spectroscopy of the different luminescence lines gives evidence of specific sets of resonances for each bound-exciton complex. Their analysis is performed based on the assumption of an exchange and crystal-field splitting of the electronic ground state of acceptor-exciton complexes in cubic ZnS. For increasing excitation densities, bound excitons remain important until a broadband emission begins to superimpose totally these structures at a several hundred kW/cm² light intensity, which resembles a band reported in Ref. 10 from low-resolution spectroscopy, and may be due to EHD recombination. No evidence is given of specific biexciton or exciton-exciton-collision luminescence.

II. EXPERIMENT

The samples were high-quality rods and platelets of 100–1000- μ m thickness, which were grown from the gaseous phase and were not intentionally doped. X-ray investigations have shown that all samples contain about 10% of hexagonal modification which, however, did not noticeably influence the optical spectra. Only the specifically cubic free-exciton absorption and reflection features have been observed in preinvestigations. The bound-exciton spectra were recorded under excitation with a pulsed dye laser pumped by an excimer laser (Lambda Physik). This system can be effectively used for intensity-dependent excitation spectroscopy. The spectral half-width of the dye laser amounts to less than 0.005 nm, with 15-ns pulse duration and pulse intensities of more than 20 MW/cm² maximum. The required emission wavelengths of 310–330 nm were obtained by frequency doubling with a potassium dihydrogen phosphate (KDP) crystal, whose beam aberration was automatically corrected by a computer-driven compensator optic. The efficiency of frequency doubling was 3% so that a maximum intensity of 600 kW/cm² was reached. The detected light was decomposed by a 0.75-m double monochromator with 0.008-nm resolution (Spex Industries) and was

recorded with a bialkali photomultiplier to yield highest resolution.

III. EXPERIMENTAL RESULTS

A. Luminescence spectra

Figure 1 shows the luminescence spectra of an undoped cubic ZnS sample between the weak emission of the free-*A* exciton (3.80 eV) and 3.73 eV, i.e., the whole energy range for which bound-exciton emission is expected. The crystal was excited with laser light of an energy above the band gap of 3.83 eV, and the spectra were taken for a backward configuration. Sets of lines I_i are visible in the spectra, whose notation is chosen in a way such that the subscripts of those lines which have also been described in Ref. 7 correspond to the subscripts given therein (X_i), whereas the notation I for bound-exciton emission lines is used in nearly all other II-VI compound semiconductors. At lowest densities (3 kW/cm²), the I_{3a} line is the most pronounced feature, and is accompanied by a high-energy structure I_{3b} . Around 10 meV higher in energy, a doublet I_{5a}/I_{5b} is visible. On the low-energy side of I_{3a} , an emission band shows up which is only poorly structured. The lines I'_1 , I_1 , and I_2 are recognized to always appear even for different luminescence spectra which have been compared.

The I_{5a}/I_{5b} doublet becomes the dominant structure in intentionally *J*-doped samples, whereas I_{3a} and I_{3b} get very weak in these luminescence spectra (Fig. 2). While I_{5b} now is a little stronger in relation to I_{5a} , the sharpness of both lines remains as is in the undoped sample. The free-exciton emission *A* is not influenced by the doping. The nature of the impurity center related to the *J* doping is discussed in Sec. IV.

The strongest luminescence lines are accompanied by the LO-phonon replicas I_{3a} -LO and I_{3b} -LO. The replica

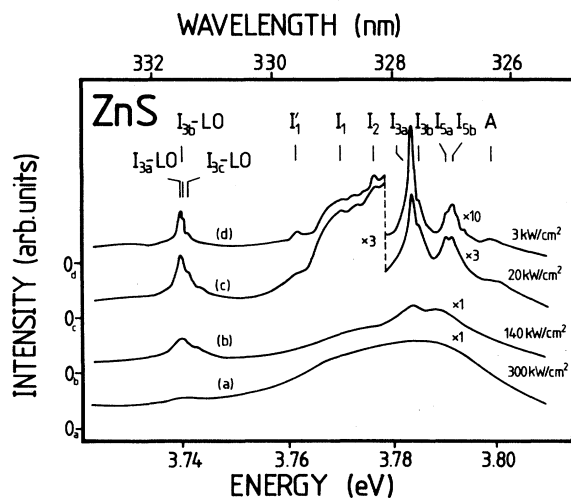


FIG. 1. Luminescence of cubic ZnS in the bound-exciton energy regime for different excitation intensities: (a) 300, (b) 140, (c) 20, and (d) 3 kW/cm². Excitation energy is above the band gap of 3.83 eV.

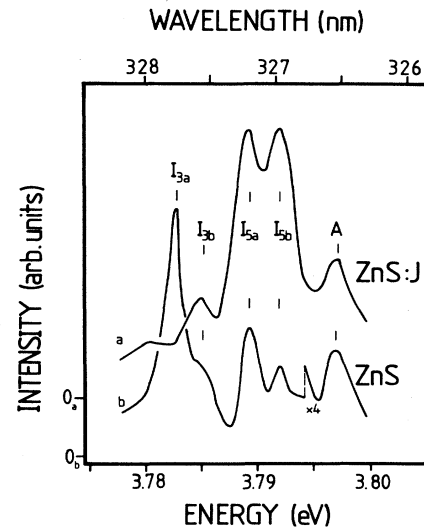


FIG. 2. Luminescence of a *J*-doped ZnS:*J* sample (upper curve) in comparison with a pure sample (lower curve). For explanations see text.

distances of 43.7 and 43.8 meV fit the LO phonon energies reported for cubic ZnS in literature quite well.¹² A weak structure I_{3c} -LO being always present does not possess a noticeable corresponding zero-phonon line. This may be due to the nearby I_5 zero-phonon line set which may be superimposed on any weak I_{3c} emission. No phonon replicas of I_{5a}/I_{5b} have been detected, most probably due to the weakness of these lines. All luminescence lines are presented in Table I.

For increasing excitation densities, these sharp lines become broadened and more and more superimposed by an extended band with a maximum energy of 3.78–3.79 eV, near the I_{3a} peak energy. At about 300 kW/cm², this band completely dominates the spectrum [see spectrum (a) of Fig. 1], and bound-exciton structures are hardly seen. No additional bands, which would resemble the biexciton *M* or exciton-exciton-collision *P* bands in CdS, CdSe, or ZnO, are visible in cubic ZnS.

B. Excitation spectra and scattering phenomena

Excitation spectra of the strongest lines I_{3a} and I_{5a} have been taken with the electric field vector $E \parallel [001]$. They exhibit the free-*A*-exciton resonance as a very pronounced common maximum, and a high-energy band at about 3.805 eV as well (Fig. 3). On the low-energy side of *A*, both lines possess two specific resonances, which, however, show a similar feature. Since the energy spacing of the first resonance relative to I_{3a} is identical to that between the I_{3a} and I_{3b} luminescence lines, and the same is valid with regard to the I_5 excitation resonances and luminescence lines, the resonances are labeled according to the luminescence nomenclature, i.e., $I_{3b,c}$ and $I_{5b,c}$. The measured spacings between the luminescence lines and excitation resonances, respectively, are presented in Table II. The intensity ratios are 2.2:2 for $I_{3b}:I_{3c}$ and 2.4:2 for $I_{5b}:I_{5c}$.

TABLE I. Luminescence lines of bound-exciton complexes in ZnS in comparison with data of other authors. The energies given in Ref. 7 have to be read taking into account that, except from I_{3a} , only weak shoulders have been found and quantitatively analyzed.

Line	Wavelength (nm)	Energy (eV)	E_B (meV)	Energy ^a (eV)	Energy ^b (eV)
A	326.28	3.8000		3.800	3.801
I_{5b}	326.994	3.7917	8.3		I_D : 3.792
I_{5a}	327.082	3.7907	9.3	3.789	
I_{3b}	327.585	3.7848	15.2	3.786	
I_{3a}	327.686	3.7837	16.3	3.784	
I_2	328.332	3.7762	23.8	3.778	
I_1	328.880	3.7699	30.1	3.771	
I'_1	329.598	3.7617	38.3		
I_{3c} -LO	331.240	3.7431			
I_{3b} -LO	331.420	3.7410		3.743	
I_{3a} -LO	331.510	3.7400		3.740	

^aReference 7.

^bReference 9.

The same set of excitation resonances, $I_{3b,c}$, with a corresponding intensity ratio to that given above, plus an additional peak at I_{3a} , is observed in the excitation spectra of I_{3a} -LO (Fig. 4), which underscores the fact that these resonances are of a very characteristic nature for each luminescence line and thus for the correlated complex. In the case of the excitation spectrum of I_{3a} -LO, the ratio of the resonances $I_{3b}:I_{3c}$ is 2.8:2. The resonance I_{3a} , however, is superimposed by the simple LO Raman replica of the laser. If the intensity of this replica is measured off resonance but near I_{3a} -LO, and is deducted from the apparent I_{3a} resonance intensity in Fig. 4, a real intensity ratio is 1:2.8:2 is obtained for $I_{3a}:I_{3b}:I_{3c}$.

The intensity dependence of the luminescences excited

via both the b and c resonances is totally coincident. As an example, that of I_{3a} is depicted in Fig. 5. After a sub-linear increase until 0.6 kW/cm^2 , the I_{3a} luminescence grows linearly when excited via $I_{3b,c}$ up to 4 kW/cm^2 . For even higher densities, a change into a saturation behavior is observed. This intensity behavior compellingly underscores the nature of $I_{3a,b,c}$ as transitions into bound-exciton states. The sublinear part for lowest densities is a generally known phenomenon of bound-exciton transitions and has been explained, e.g., by competing impurity luminescence processes in this intensity range.⁶⁻⁸ Linearity and saturation due to the restricted number of centers is a typical physical property of optical bound-exciton creation.

For certain geometries and increased excitation intensities, the luminescence feature in the I_3 line set range is additionally superimposed by scattering lines S_{3b} and

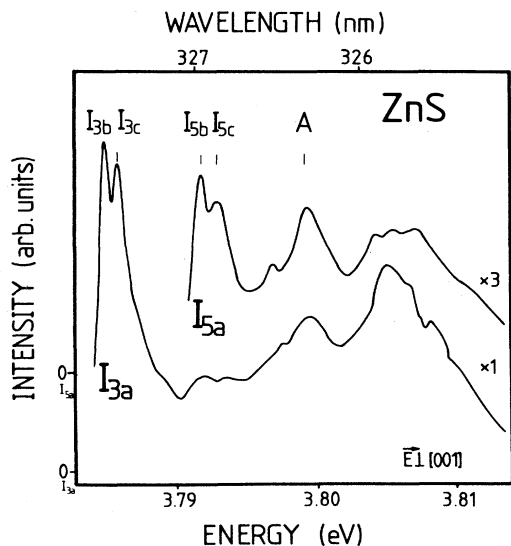


FIG. 3. Excitation spectra of I_{3a} and I_{5a} for an excitation density of 5 kW/cm^2 .

TABLE II. Absolute energies and energy spacings of the luminescence lines and excitation resonances $I_{3a,b,c}$ and $I_{5a,b,c}$. In the column describing the appearance of structures, L denotes "appearance as luminescence line," and E denotes "appearance as excitation maximum."

Line name	Appearance as	Energy (eV)	Spacing to I_{5a} , I_{3a} , or I_{3a} -LO resp. (meV)
I_{5a}	L, E	3.7907	
I_{5b}	L, E	3.7917	0.9
I_{5c}	E	3.7926	1.9
I_{3a}	L, E	3.7837	
I_{3b}	L, E	3.7851	1.4
I_{3c}	E	3.7863	2.6
I_{3a} -LO	L	3.7400	
I_{3b} -LO	L	3.7410	1.0
I_{3c} -LO	L	3.7431	3.1

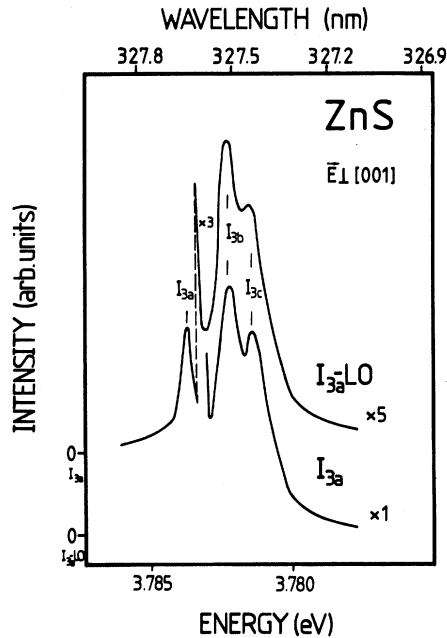


FIG. 4. Excitation spectrum of I_{3a} -LO in direct comparison with that of I_{3a} for an excitation density of 2 kW/cm^2 .

S_{3c} , which show a resonance maximum if they, subsequently, exactly coincide with the I_{3a} peak (Fig. 6). This is the case only when the laser is tuned on the I_{3b} or I_{3c} excitation maximum, respectively. If the laser is detuned from these values, the scattering lines are shifted from I_{3a} and become weak, and soon are hardly detectable in the spectra. Although these scatterings lines may disturb the recording of excitation spectra of the luminescence lines when becoming coincident with them, their intensities are weak, especially for lower excitation intensities. Thus, the analysis of the excitation spectra is not seriously hindered if care is taken to minimize the influence of

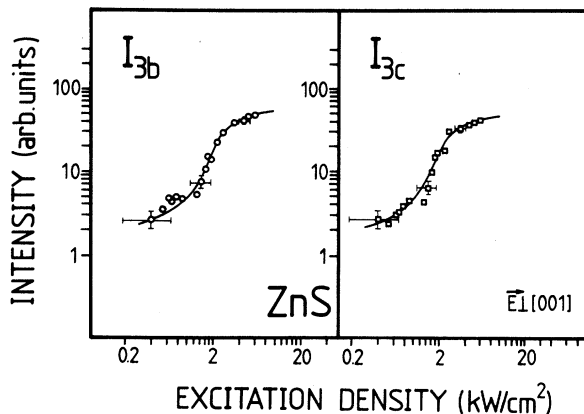


FIG. 5. I_{3a} luminescence intensity for excitation via I_{3b} (left-hand side) and I_{3c} (right-hand side) as function of the excitation density.

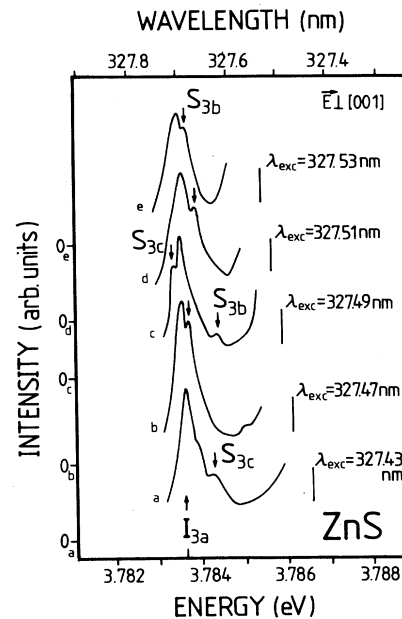


FIG. 6. Raman scattering lines S_{3b} and S_{3c} in the I_3 line set regime for different laser wavelengths.

the scattering lines. Moreover, their immediate connection with the excitation resonances is obvious. However, the line's Stokes shifts are not constant. Only when they are on resonance are they equal to the resonance's spacings in relation to the luminescence line I_{3a} . In Fig. 7, they are shown to increase by 0.6 meV per meV decrease of the laser energy. However, it is interesting to notice that the mutual distance of the two scattering lines remains nearly constant. In the I_5 line's energy range, a corresponding scattering phenomenon is observed; however,

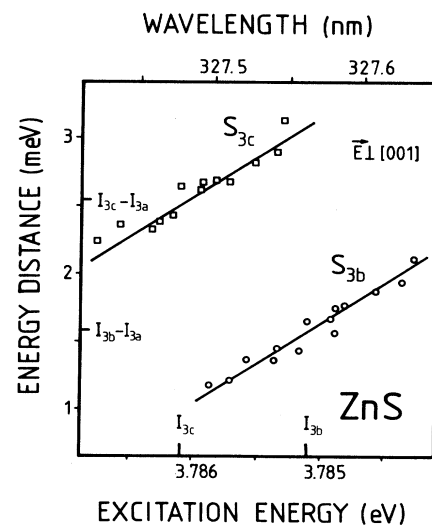


FIG. 7. S_{3b} and S_{3c} Raman line Stokes shifts as function of the laser wavelength. I_{3b} and I_{3c} denote the energies of the excitation maxima.

the Raman lines are much weaker, and thus could not be analyzed in detail.

IV. DISCUSSION

According to Table I, the bound-exciton binding energies have been found to range from 8.3 to 38.3 meV in cubic ZnS. The doublet I_{5a}/I_{5b} lies at about the energy for which Taguchi *et al.*⁹ detected a line I_D and assigned it to a neutral-donor-exciton complex. However, a definite decision as to which kind of bound-exciton complex a luminescence line belongs requires the analysis of any expected term's fine structure.

The specific excitability of I_{3a} via $I_{3b,c}$ and I_{5a} via $I_{5b,c}$ shows that these sets of three lines each have to be interpreted as belonging to one complex, respectively. Since the energy spacings of $I_{3b,c}$ and $I_{5b,c}$ in relation to I_{3a} and I_{5a} , respectively, amount only to 1–2 meV, it can be excluded that the $I_{ib,c}$ resonances or lines are transitions into or from excited electronic states of the complexes giving rise to the I_{ia} luminescence lines. Such an excited electronic state has to be expected to lie much higher above the bound state. This has been shown for donor-exciton and acceptor-exciton complexes in ZnTe (Ref. 4) and in the wurtzite-structured compounds CdS (Ref. 3) and ZnO,⁵ which possess binding energies on the same order of magnitude as the complexes treated here to appear in ZnS. Thus, excitation resonances due to a fine-structure splitoff of the electronic ground state is a more reasonable explanation to be further discussed. For the donor-exciton complex (D^0, X) in cubic ZnS (zinc blende, point group T_d), the two like Γ_6 electrons involved in such a system are only allowed to pair antiparallel. The remaining Γ_8 hole gives rise to a single $j = \frac{3}{2}$ (D^0, X) ground state.¹⁴ Thus, no fine structure of this state is expected.

This situation changes with regard to an acceptor-exciton complex (A^0, X) in ZnS. As has been generally shown for zinc-blende-structured crystals,¹³ the two Γ_8 holes ($j = \frac{3}{2}$) are only allowed to couple to combinations of antisymmetric wave functions with a total $J=0$ and 2. These two states are split by hole-hole interaction. If the electron is coupled to the holes, a Γ_6 ($j = \frac{1}{2}$) state results from $J=0$, and states Γ_8 ($j = \frac{3}{2}$) and $\Gamma_7 + \Gamma_8$ ($j = \frac{5}{2}$) are obtained from $J=2$ in a crystal field of T_d symmetry. The $\Gamma_7 + \Gamma_8$ degeneracy can be lifted by electron-hole interaction which, however, is very small in most cases.^{14,15} This fine structure is well established, e.g., for GaAs (Ref. 14) and CdTe.¹⁵ Normally, the states resulting from $J=2$ should be of lower energy than the $j = \frac{1}{2}$ level.¹³ However, in particular, acceptors of considerable ionization energy (more than about 100 meV) cause pronounced hole-attractive central-cell corrections, pulling the $J=0$ correlated state below the $J=2$ correlated levels, since the first one is more sensitive to these modifications.¹⁴ Thus, the experiment has to show from case to case which term sequence of Γ_6 , Γ_8 , and $\Gamma_7 + \Gamma_8$ is valid for an observed (A^0, X) complex. The multiplet feature of the I_3 and I_5 line sets in luminescence as well as in excitation indicates that they belong to acceptor-exciton complexes rather

than to donor-exciton systems. Thus, if such acceptor centers are assumed to be correlated with the I_3 and I_5 lines, respectively, the term scheme depicted in Fig. 8 is obtained. All experimental data are in best agreement with this suggestion, if the lowest-energy lines I_{3a} and I_{5a} are assigned to the transitions from or into the lowest-lying Γ_6 levels of the two different (A^0, X) complex, I_{3b} and I_{5b} , respectively, to those from or into the $\Gamma_7 + \Gamma_8$ levels, and I_{3c} and I_{5c} to those from or into the highest-lying Γ_8 levels. As in other known cases,^{14,15} the electron-hole interaction is too small to measurably split the $\Gamma_7 + \Gamma_8$ levels. It has been shown by theoretical analysis^{15,16} that a straightforward calculation, using a Hamiltonian constructed of a parametrized electron-hole and crystal-field contribution, yields two limiting cases of expected oscillator strengths of transitions into electronic levels of bound excitons in cubic semiconductors; one for the electron-hole interaction being much stronger than the crystal-field influence, the other for the reverse situation. Since we have to deal with the latter case of a small electron-hole-exchange coupling compared to the crystal-field splitting, the levels are split into the above-mentioned states Γ_6 , $\Gamma_7 + \Gamma_8$, and Γ_8 . The theoretical oscillator-strength ratio for unthermalized transitions from the acceptor ground state into these levels is 1:3:2. This corresponds quite well to the registered ratios $I_{ia}:I_{ib}:I_{ic}$ in the excitation spectra, best measurable for I_{3a} -LO, where a ratio of 1:2.8:2 is obtained if the laser LO Raman line intensity is subtracted from the I_{3a} resonance intensity. Concerning the luminescence spectra, the usual exponential thermalization law for the measured energy spacings of the levels must in addition be taken into account for the two complexes. The measured ratios of 4:1:0 for $I_{3a}:I_{3b}:I_{3c}$ and 1.2:1:0 for $I_{5a}:I_{5b}:I_{5c}$ (the 0 stands for the undetectable I_{3c} and I_{5c} lines) are as expected if thermalization and oscillator-strength rules are combined for a crystal temperature of around 5 K. Only the $I_{5a}:I_{5b}$ ratio is a little larger than calculated. However, since the exact ratio of luminescence line intensities depends sensitively on crystal temperature influenced by the laser, especially for high pulse intensities (see, e.g., the slightly changed $I_{5a}:I_{5b}$ ratio of the J -

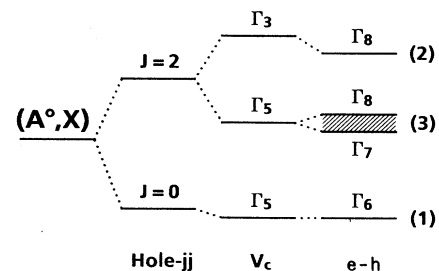


FIG. 8. Term scheme of the acceptor-exciton complex in its electronic ground state. Hole- jj denotes the influence of the hole-hole interaction, V_c that of the crystal field, and $e-h$ the electron-hole interaction which splits the Γ_5 level into Γ_7 and Γ_8 . However, this energy spacing is not measurable in the experiment. In parenthesis, the experimentally observed relative oscillator strengths of transitions between the A^0 ground state and the levels shown are given.

doped sample, Fig. 2), the more reliable results are obtained from the excitation resonances, which are independent of slight temperature changes.

Besides the transitions' intensity ratios, the term ordering Γ_6 (lowest), $\Gamma_7 + \Gamma_8$, and Γ_8 is favored by the measured energy spacings of the two I_3 and I_5 line sets as well. The hole-hole split corresponds to the energy distance between the "a" lines and the center of the respective "b" and "c" doublets. It is calculated to be 1.4 meV for the I_5 lines and 2.0 meV for the I_3 lines, and thus sensitively decreases with the decreasing binding energy of the acceptor-exciton complex involved, i.e., increasing interparticle distance, in accordance with theoretical expectation. The crystal-field splitting is directly obtained by the "b"- "c" spacing of 1.0 meV for the I_5 set and 1.2 meV for the I_3 set, and thus is nearly unaffected by the binding energy, i.e., the interparticle distance within the complex. These values underscore the given term order and are very reasonable when compared with theory¹⁴ and experimental observations on other zinc-blende compounds^{15,16} (Table III).

This assignment of the observed transitions is even more underscored by the observation of the luminescence enhancement of I_{5a}/I_{5b} when the crystal is J doped. It is well known that the halogenides in II-VI compounds give rise to the formation of acceptor centers if they are combined with a double acceptor, usually a chalcogenide vacancy.¹⁷ Consequently, a $(V_{Zn}^{2-}J_S^+)^-$ acceptor center is expected to be created in ZnS, since the $I_{5a}/I_{5b}/I_{5c}$ luminescences and excitation resonances unambiguously show the features of an acceptor-exciton complex.

The given interpretation is strongly supported by the observation of the low-energy shift of the S_3 scattering lines' Stokes energies for increasing excitation energy. We explain the scattering phenomena as an electronic Raman process, where the virtual excitation of an acceptor-exciton complex in one of the fine-structured states is followed by a very fast relaxation into the lowest Γ_6 level and zero-phonon or LO-phonon (I_{3a} -LO energy range) -assisted reemission. If so, it becomes quite understandable that such a process is resonant at the three discussed energy levels, and becomes very weak off-resonance. For increasing laser energies, the virtually created acceptor-exciton complexes, naturally, correspond to systems of lower total binding energies, which result in increased spatial extension and thus reduced interparticle interaction. Therefore, the Stokes shifts

which represent the splitoff of the fine-structure levels due to hole-hole interaction show a pronounced decrease. Just the opposite is the case for decreasing laser energies and thus increasing complex binding energies. The mutual S_{3b} - S_{3c} distance represents the crystal-field influence, as does the spacing of the corresponding excitation resonances, and remains nearly constant for tuned laser energies. This shift behavior of electronic Raman scattering at bound-exciton complexes is in accordance with observations at an acceptor-exciton system in CdS,¹ and provides valuable additional information on the properties of bound-exciton complex in ZnS, supporting the model discussed above.

In the luminescence spectra, the bound-exciton transitions are demonstrated to play the most important role up to intensities of some tens of kW/cm². No characteristic biexciton or exciton-exciton-collision band is shown up in this excitation density range. This may indicate that biexcitons do not exist in cubic ZnS. In Ref. 18, the biexciton binding energy was calculated to be 2.8 meV maximum. Obviously, this small value is even overestimated.

Instead of biexciton luminescence, a very broad band emerges for about 100 kW/cm² which covers the whole bound-exciton regime. This band agrees well in peak energy and structure with the emission observed in Ref. 10. However, the initial sharp line at 3.80 eV, reported therein as bound-exciton luminescence, obviously is free-exciton emission, whereas no bound-exciton luminescence is resolved in those considerably broadened spectra. The given explanation of the band as electron-hole-drop (EHD) decay is of a rather hypothetical nature, but, indeed, this band is much too broad to be correlated with biexciton or multiexciton processes, and its feature corresponds to the calculated one (see Refs. 10 and 11). Since an EHD has been estimated to remain stable in cubic ZnS up to temperatures of several tens of K, this explanation is the most promising up to now. However, further investigations of the band's properties are necessary.

V. SUMMARY AND CONCLUSIONS

In conclusion, we interpret the transition sets I_{3a} , I_{3b} , and I_{3c} on the one hand, and I_{5a} , I_{5b} , and I_{5c} on the other hand each as being due to luminescence form or excitation into the threefold fine-structured electronic ground

TABLE III. Hole- jj splitting $\Delta E(jj)$, crystal-field splitting $\Delta E(V_c)$, and electron-hole splitting $\Delta E(e-h)$ for the analyzed acceptor-exciton complexes in cubic ZnS, in comparison with data for acceptor-exciton complexes in other zinc-blende compounds.

	I_3 set	I_5 set	CdTe:Cu ^a	Si:In ^b	Si:Ga ^b
$\Delta E(jj)$ (meV)	2.0	1.4	1.2	4.7	1.3
$\Delta E(V_c)$ (meV)	1.2	1.0	0.4	3.2	0.3
$\Delta E(e-h)$ (meV)			0.02		

^aReference 15.

^bReference 16.

states of two acceptor-exciton complexes involving different acceptor centers. The I_5 line set is correlated with a J doping; most probably it exhibits an acceptor center involving a double acceptor and a donorlike J atom, as is the case in other II-VI compounds. The lines' mutual energy spacings and thermalization, their occurrence as specific excitation resonances of the I_{ia} or I_{ia} -LO luminescences, respectively, and the existence of a laser-energy-dependent scattering phenomenon gives well-founded arguments for their assignment to the (A^0, X) ground-state levels in the order Γ_6 ($j = \frac{1}{2}$), $\Gamma_7 + \Gamma_8$ ($j = \frac{5}{2}$), and Γ_8 ($j = \frac{3}{2}$). However, magneto-

optics of the luminescences, as well as of the excitation resonances, is highly desirable and in preparation to support the given interpretation.

ACKNOWLEDGMENTS

The authors wish to thank Dr. R. Broser for supplying the crystals and performing the J doping, and Dr. A. Krost for performing the x-ray analysis. This work was partly supported by the Deutsche Forschungsgemeinschaft (Bonn, Germany).

-
- ¹J. Gutowski, Phys. Rev. B **31**, 3611 (1985); J. Gutowski and I. Broser, *ibid.* **31**, 3621 (1985).
- ²J. Gutowski and I. Broser, J. Phys. C **20**, 3771 (1987), and the literature cited therein.
- ³J. Puls, F. Henneberger, and J. Voigt, Phys. Status Solidi B **119**, 291 (1983).
- ⁴Le Si Dang, A. Nahmani, and R. Romestain, Solid State Commun. **46**, 743 (1983).
- ⁵J. Gutowski, T. Hönig, N. Presser, and I. Broser, J. Lumin. **40/41**, 433 (1988); J. Gutowski, N. Presser, and I. Broser, Phys. Rev. B **38**, 9746 (1988) and the literature cited therein.
- ⁶W. Klein, J. Phys. Chem. Solids **26**, 1517 (1965).
- ⁷U. Flesch, R.-A. Hoffmann, and R. Rass, J. Lumin. **3**, 137 (1970).
- ⁸S. Geczi and J. Woods, J. Appl. Phys. **51**, 1866 (1980).
- ⁹T. Taguchi, T. Yokogawa, and H. Yamashita, Solid State Commun. **49**, 551 (1984).
- ¹⁰R. Baltrameyunas and E. Kuokshtis, Fiz. Tverd. Tela (Leningrad) **22**, 1009 (1980) [Sov. Phys.—Solid State **22**, 589 (1980)].
- ¹¹R. Baltrameyunas and E. Kuokshtis, Pis'ma Zh. Eksp. Teor. Fiz. **28**, 72 (1978); **28**, 588 (1978) [JETP Lett. **28**, 66 (1978); **28**, 542 (1978)].
- ¹²C. A. Klein and R. N. Donadio, J. Appl. Phys. **51**, 797 (1980); M. Kranzmann, C. R. Acad. Sci. **266**, 1224 (1968).
- ¹³B. Stébé and G. Munsch, Solid State Commun. **40**, 663 (1981).
- ¹⁴D. Bimberg, W. Schairer, M. Sondergeld, and T. O. Yep, J. Lumin. **3**, 175 (1970); A. M. White, P. J. Dean, L. L. Taylor, and R. C. Clarke, J. Phys. C **5**, L110 (1972); A. M. White, *ibid.* **6**, 1971 (1973); A. M. White, P. J. Dean, and B. Day, *ibid.* **7**, 1400 (1974).
- ¹⁵E. Molva and Le Si Dang, Phys. Rev. B **32**, 1156 (1985).
- ¹⁶K. R. Elliott, G. C. Osbourn, D. L. Smith, and T. C. McGill, Phys. Rev. B **17**, 1808 (1978).
- ¹⁷D. G. Thomas, R. Dingle, and J. B. Cuthbert, in *Proceedings of the International Conference on II-VI Semiconducting Compounds, Providence, 1967*, edited by D. G. Thomas (Benjamin, New York, 1967), p. 863; C. H. Henry, K. Nassau, and J. W. Shiever, Phys. Rev. B **4**, 2453 (1971).
- ¹⁸G. Beni and T. M. Rice, Phys. Rev. B **18**, 768 (1978).